

# Contrasting fungal functional groups influence nutrient cycling across four Japanese cool-temperate forest soils

Felix Seidel<sup>a,\*</sup>, Carles Castaño<sup>b,1</sup>, Josu G. Alday<sup>c,e</sup>, M. Larry Lopez C.<sup>d</sup>, José Antonio Bonet<sup>c,e</sup>

<sup>a</sup> Thünen Institute of climate-smart agriculture, Thünen Institute, Braunschweig, Germany

<sup>b</sup> Department of Forest Mycology and Plant Pathology, Uppsala BioCenter, Swedish University of Agricultural Sciences, SE-750 07 Uppsala, Sweden

<sup>c</sup> Department of Agricultural and Forest Sciences and Engineering, University of Lleida, Av. Rovira Roure, 191, 25198 Lleida, Spain

<sup>d</sup> Faculty of Agriculture, Yamagata University, Tsuruoka, Japan

<sup>e</sup> Joint Research Unit CTF-AGROTECNIO-CERCA, Av. Rovira Roure, 191, 25198 Lleida, Spain

## ARTICLE INFO

### Keywords:

Saprotrophs  
Mycorrhizal types  
Ectomycorrhiza  
Soil fungi  
N cycling

## ABSTRACT

Understanding soil dynamics and nutrient cycling is crucial for the sustainable management of Japanese forests covering 70 % of the national land area. These forests are dominated by tree species with contrasting traits, influencing soil dynamics differently. We investigated how changes in soil characteristics across different forest stands shift in composition and functioning of fungal communities. Four different forest stands dominated by two different mycorrhizal types were selected: *Fagus crenata* and *Larix kaempferi*, representing ectomycorrhizal (ECM) types, and *Cryptomeria japonica* and *Robinia pseudoacacia*, representing arbuscular mycorrhizal (AM) types. In total, 62 composite topsoil samples from two depths were analyzed for their physicochemical properties and fungal communities were profiled by DNA sequencing. Ectomycorrhizal fungi dominated soils of *Fagus crenata* and *Larix kaempferi* forests, while fungal saprotrophs were more abundant in *Cryptomeria japonica* and *Robinia pseudoacacia* forests. Forest stand type rather than soil depth determined the composition and structure of soil fungal communities. Soil pH was positively correlated with abundances of saprotrophic fungi ( $P < 0.05$ ) and negatively with ECM fungi. Soil C:N ratio was positively correlated, and nitrate was negatively correlated with relative abundances of root-associated fungi, primarily ECM fungi. No links between C nor N stocks with fungal guilds were found across the dataset. Observed links between soil C:N ratio and relative abundances of root-associated fungi and saprotrophs stress the importance of these guilds for influencing nutrient cycling economy across contrasting forest types. The lack of correlation between fungal communities and soil C and N stocks suggests distinct mechanisms driving stocks in these soils.

## 1. Introduction

Understanding the drivers that influence nutrient dynamics and carbon cycling in forest soils is crucial to elaborate efficient forest management policies aiming to keep the broadest range of ecosystem services. Nitrogen (N) and carbon (C) dynamics in forest soils are tightly linked to the activity of soil microorganisms, particularly soil fungi and bacteria (DeBellis et al., 2007; Hagenbo et al., 2022). Fungal saprotrophs decompose litter and transform organic matter into plant-available nutrients (Baldrian et al., 2011; Dighton, 2003), while mycorrhizal fungi provide physical protection against pathogens and facilitate access to soil nutrients by establishing symbiotic relationships with trees (Cairney, 2012; Smith and Read, 2008; Cairney, 2012). Particularly, tree

access to N bound in organic forms is tightly dependent on ectomycorrhizal or ericoid mycorrhizal fungi (Lilleskov et al., 2002; Smith and Read, 2008). By contrast, arbuscular mycorrhizal fungi have limited capability to access organic N (Smith and Read, 2008). Despite these differences in nutrient acquisition strategies among mycorrhizal fungi, we still lack knowledge of the mechanisms behind the links between the types of mycorrhiza and soil C and N cycling and stocks.

Trees can be classified by the type of mycorrhizal fungi to which they associate, mainly arbuscular mycorrhizal (AM), ectomycorrhizal (ECM), or ericoid mycorrhizal (ERM) fungi (Smith and Read, 2008). These so-called mycorrhizal types have been shown to differently affect organic matter dynamics and soil characteristics in forest soils (Averill et al., 2014; Phillips et al., 2013; Zhu et al., 2018). Across mycorrhizal types,

\* Corresponding author at: Thünen Institute of Climate-smart Agriculture, Bundesallee 50, 38116 Braunschweig, Germany.

E-mail address: [felix.seidel@thuenen.de](mailto:felix.seidel@thuenen.de) (F. Seidel).

<sup>1</sup> These authors contributed equally.

MANE (“mycorrhiza-associated nutrient economy”) framework predicts that soil organic N cycling prevails in ECM types, which are characterized by low nitrification rates and low inorganic N relative to organic N (Phillips et al., 2013). By contrast, soil inorganic N cycling and nitrification processes dominate in AM types, which are typically dominated by saprotrophs and AM fungi (Lin et al., 2017; Phillips et al., 2013). Shifts from inorganic towards organic nitrogen cycling can often be reflected with increases in averaged soil C:N ratios (Averill et al., 2014; Phillips et al., 2013; Zhu et al., 2018) or depth-wise soil C:N ratios (Castaño et al., 2023; Clemmensen et al., 2021). Thus, in general, topsoils under ECM types have higher C:N ratios than AM types (Averill et al., 2014; Heděnec et al., 2020; Zhu et al., 2018), but how this translates in the total soil C and N stocks remains unclear.

Fungal communities in forest soils are compartmentalized with soil depth according to variations in soil organic matter characteristics. Thus, often the topmost soil layer is dominated by fungal saprotrophs, while root-associated fungi often dominate the deeper soil layers with more decomposed organic matter (Andretta et al., 2011; Jumpponen et al., 2010; Lindahl et al., 2007; Mundra et al., 2021; Voříšková et al., 2014). Availability of soil N in forests influences the outcome of competitive interactions among fungi (Sterkenburg et al., 2018) and is related to variation in soil processes such as organic matter decomposition (e.g. via gadgil effects, Fernandez and Kennedy, 2016) and soil C storage (Soudzilovskaia et al., 2019). ECM can inhibit decomposition processes by competing for organic substrates with fungal saprotrophs (Averill, 2016) or retaining large amounts of N in their mycelia (Näsholm et al., 2013). However, certain ECM fungi can also efficiently access organic N, which can result in a release of soil C (Clemmensen et al., 2013, 2015; Lindahl and Tunlid, 2015). Saprotrophic dominance typical of AM types can also enhance decomposition processes, and potentially reduce soil C stocks (Averill et al., 2014; Averill, 2016). Consequently, mycorrhizal types not only may determine soil and plant nutrient cycling but also potentially soil C and N stocks via competitive interactions between fungal guilds.

Over 70 % of Japan is covered by forests, many of which harbour native species with limited global geographical distribution such as *Fagus crenata* (*F. crenata*), *Cryptomeria japonica* (*C. japonica*), and *Larix kaempferi* (*L. kaempferi*). Information on soil fungal communities in Japanese forests remains mostly limited to the temperate forests of Kanto region (An et al., 2008; Miyamoto et al., 2014; Nara, 2006; Ochimaru and Fukuda, 2007; Shigyo et al., 2019), particularly in ice-age relict forests (Koizumi et al., 2018; Koizumi and Nara, 2020) or in the dunes of Tottori (Taniguchi et al., 2007), while studies conducted in cool temperate forests of Japan are exiguous (Ishida et al., 2007; Fukasawa et al., 2009). Thus, profiling of the soil fungal communities inhabiting these forests is essential to better understanding microbial-driven dynamics of nutrient cycles in Japanese cold temperate forests (Ishida et al., 2007). Particularly, the soil microbiome of *C. japonica* and *L. kaempferi* have been rarely profiled although they are widely used species for commercial purposes in Japan. These two species as well as the typical cool temperate tree species *F. crenata* and the highly invasive *Robinia pseudoacacia* (*R. pseudoacacia*) differ in the type of mycorrhizal fungi they associate; *F. crenata* and *L. kaempferi* establish symbiotic associations with ECM fungi while *C. japonica* and *R. pseudoacacia* form AM associations, suggesting that soil nutrient cycling and element stocks between these two species may differ. In addition, N uptake in *R. pseudoacacia* is also enhanced by root nodulation of bacteria in the subclasses *Gammaproteobacteria* and *Betaproteobacteria*.

Based on these premises, we collected 62 composite soil samples from distinct ECM (*F. crenata* and *L. kaempferi* forest stands) and AM (*C. japonica* and *R. pseudoacacia* forest stands) types in a cold-temperate forest area in Japan. We aimed to describe the soil fungal communities in these stands and assess their relationships with soil organic matter characteristics and C and N stocks at two different soil depths. We hypothesized that (1) soil fungal communities would differ among forest stands and especially between mycorrhizal types, based on the MANE

framework (Phillips et al., 2013), but also between soil depths, considering the functional compartmentalization of fungi with soil depth (Freya et al., 2021). (2) Changes in soil fungal communities would be linked to nutrient cycling patterns (organic vs. inorganic), as reflected by differences in inorganic N and soil C:N ratios, with expected higher soil C:N ratios and lower inorganic N in ECM types (*F. crenata* and *L. kaempferi*, Enta et al., 2020) compared to AM types (*C. japonica* (Matsuda et al., 2021) and *R. pseudoacacia*; (Yang et al., 2015)). (3) As a consequence of the distinct nutrient cycling patterns, soil C stocks are expected to be greater in ECM types compared to AM types, due to greater C losses mediated by saprotrophs in AM types.

## 2. Materials and methods

### 2.1. Study site

The study area is located in the Research Forest of Yamagata University in north-eastern Japan (N38° 32.889' E139° 51.706', Fig. 1), covering approximately 3 km<sup>2</sup>. The elevation of the study sites ranged from 300 to 700 m above sea level. The mean annual temperature is 9.7 °C and annual precipitation is 2558 mm of which half is snow, thus representing a system with high-water availability. All soils in the forest stands were identified as haplic Cambisols (FAO, 2006).

Four forest stands were chosen based on dominant tree species with contrasting mycorrhizal types. Specifically, we chose two tree species that establish associations with ECM fungi (*Fagus crenata* Blume and *Larix kaempferi* Lamb.) and two species that establish associations with AM fungi (*Cryptomeria japonica* D. Don. and *Robinia pseudoacacia* L.). In addition to AM associations, *R. pseudoacacia* roots also establish symbiotic relationships with N-fixing bacteria. In total, 10 plots were established randomly over the forest stands selected: i) three plots covered by 70-year-old *F. crenata*, ii) three plots dominated by 50-year-old *L. kaempferi* (> 80 %), and iii) three plots covered by 50-year-old *C. japonica* plantations. Finally, we included a single plot with 7-year-old *R. pseudoacacia*, which was once covered by a *C. japonica* plantation that was harvested and subsequently burned and was the only area in the research forest where this species is currently found.

### 2.2. Sample collection

Soils were sampled at the beginning of August 2017 for chemical analyses. In each of the plots, trees of similar age, diameter at breast height, and total height were selected; *F. crenata* (3 trees in 3 plots, total sampled trees  $n = 9$ ), *L. kaempferi* (3 trees in 2 plots and 2 trees in a third plot, total sampled trees  $n = 8$ ), *C. japonica* (3 trees in 3 plots, total sampled trees  $n = 9$ ), *R. pseudoacacia* (5 trees in 1 plot, total sampled trees  $n = 5$ ) (for additional information see Seidel et al., 2019a, 2019b, 2022) resulting in a total of 31 selected trees. Three soil pits around each individual tree were dug by shovel and sampled within 30 cm distance. Topsoil samples were taken after removal of the litter layer from two fixed depths (0–5 cm, 5–15 cm). In the same pits, the bulk density was assessed using the core method (Al-Shammmary et al., 2018). All samples were taken from the field in a cooler box, air-dried for at least 48 h and then sieved (< 2 mm). Subsequently, samples from the three pits around each tree were pooled according to their depth, grounded, and stored in a fridge until further analysis. Samples used for the determination of inorganic N were frozen after transport from the field and stored in the dark. Before analysis, they were thawed overnight in a refrigerator, sieved (< 2 mm), and pooled.

Soil samples were collected in the same forest stands in May 2018 for fungal analyses. Four soil cores (8 cm in diameter) were taken around each tree in each cardinal direction 1 m from the trunk at two distinct depths excluding the organic layer: 0–5 cm (top) and 5–15 cm (bottom). All soil samples were taken from the field in a cooler box, freeze-dried for at least 48 h, and then sieved (< 2 mm). Subsequently, samples of each tree were pooled preserving soil stratification, homogenized, and

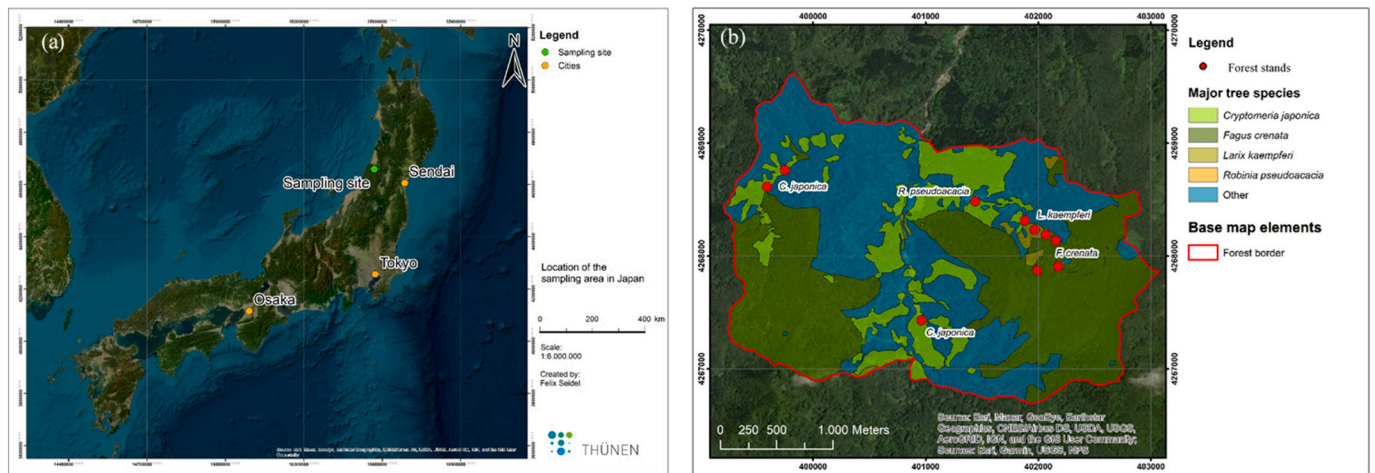


Fig. 1. (a) Location of the sampling site in Japan (b) Map of the forest stands of *Fagus crenata* (Blume), *Larix kaempferi* (Lamb.), *Cryptomeria japonica* (D. Don.) and *Robinia pseudoacacia* (L).

stored in a freezer ( $-20\text{ }^{\circ}\text{C}$ ) until DNA extraction.

### 2.3. Soil texture and chemical analysis

Soil texture was determined in triplicate with a laser diffraction particle size analyzer (Coulter LS200 with an attached Fluid Module, Beckman Coulter GmbH, Germany), after treating the samples with  $\text{H}_2\text{O}_2$  and  $\text{Na}_4\text{P}_2\text{O}_7$ . pH was determined in a 1:2.5 soil: water suspension. Total C and N contents were analyzed by dry combustion using SUMIGRAPH NC-220F automatic highly sensitive NC analyzer SCAS (Japan). For the determination of  $\delta^{15}\text{N}$  in the soil, a Thermo Quest EA1110 Elem to Nitrogen (N) I Analyzer (Italy) connected to an IsoPrime (GV Instruments UK) was used.

Total soluble N ( $\text{TN}_b$ ) and total organic C (TOC) were extracted from the soil samples by shaking them with 50 ml of 1 M KCl. Supernatant was centrifuged, filtered (0.45  $\mu\text{m}$ ), and stored in a refrigerator until subsequent analysis with a TOC/ $\text{TN}_b$  analyzer (vario TOC cube, elemental, Germany) for  $\text{TN}_b$  determination. Ammonium content was determined using the method of Crooke and Simpson (1971), whereas nitrate content was determined by using the method of Mulvaney (1996) modified by Miranda et al. (2001). Colorimetric determination of ammonium and nitrate content was conducted with a U-2000 Spectrophotometer (Hitachi, Japan). Dissolved organic nitrogen (DON) in the extracts was calculated as follows:

$$\text{DON} = \text{TN}_b - (\text{NH}_4^+ + \text{NO}_3^-).$$

Olsen extractable P was extracted following Olsen et al. (1954) and determined colorimetrically using malachite-green (Kuo, 1996).

### 2.4. Soil DNA extraction and DNA sequencing

From the homogenized soil samples for fungal analysis genomic fungal DNA was extracted from 0.350 mg of dry soil with the NucleoSpin® soil kit (Macherey-Nagel, Duren, Germany) following the manufacturers' protocol.

The Internal Transcribed spacer 2 (ITS2) region of the rRNA gene was amplified with a Mastercycler® nexus X2 (Eppendorf, Germany) using the fungal-specific Forward gITS7 and reverse ITS4 (Ihrmark et al., 2012) and reverse ITS4arch (Sterkenburg et al., 2018) primers, in which unique 8-bp tags differing in at least three positions were fitted. PCR of each sample was optimized to reduce length biases during PCR (Castaño et al., 2020), with most samples amplifying well between 26 and 28 cycles. Samples were amplified in triplicates and negative controls were included. Final concentrations in the 50  $\mu\text{l}$  PCR samples were: 25 ng

template in 25  $\mu\text{l}$ , 200  $\mu\text{M}$  of each nucleotide in 5  $\mu\text{l}$ , 2,75 mM  $\text{MgCl}_2$  in 1.5  $\mu\text{l}$ , Primers, at 0.5, 0.3, 0.15  $\mu\text{M}$  for the gITS7, ITS4 and ITS4arch, respectively, in 5  $\mu\text{l}$ , 0.025 U  $\mu\text{L}^{-1}$  polymerase (DreamTaq, Thermo Scientific, USA) in 0.25  $\mu\text{l}$ , and 1 $\times$  buffer PCR in 5  $\mu\text{l}$ . PCR conditions were as follows: 5 min at  $95\text{ }^{\circ}\text{C}$ , followed by 26–28 cycles 30 s at  $95\text{ }^{\circ}\text{C}$ , 30 s at  $56\text{ }^{\circ}\text{C}$ , 30 s at  $72\text{ }^{\circ}\text{C}$ , and a final extension step at  $72\text{ }^{\circ}\text{C}$  for 7 min. Amplicons were purified with the AMPure kit (Beckman Coulter Inc., USA) and quantified using a Qubit fluorometer (Life Technologies, USA). From each sample, equal amounts of DNA were pooled and purified using the EZNA Cycle Pure kit (Omega Biotek). Quality control of the purified samples was conducted using a BioAnalyzer 2100 (Agilent Technologies, USA) and a 7500 DNA chip. The DNA library was sequenced using the Illumina MiSeq platform, with 300-bp paired-end read lengths, generating 1.5 M sequences. Samples were sent for sequencing to the Centre for Genomic Regulation (CRG) Barcelona, Spain using Illumina MiSeq (2  $\times$  300 cycles).

### 2.5. Bioinformatic analyses

The resulting ITS2 sequences were screened for quality control and sequence clustering using the SCATA pipeline (<https://scata.mykopat.slu.se/>). ITS2 sequences with <200 bp were removed, with an average quality score < 20, or containing individual bases with a quality score < 10 were removed, and remaining sequences were screened for primers (requiring 90 % primer match) and sample tags. After collapsing homopolymers to 3 bp, sequences were clustered into species-level operational taxonomical units (OTUs) using single-linkage clustering (USEARCH; Edgar, 2010) with a threshold distance to the closest neighbor of 1.5 % (Lindahl et al., 2013). Pairwise alignments were scored using a mismatch penalty of 1, gap open penalty 0 and a gap extension penalty 1.

### 2.6. Taxonomic and functional identification

The 600 most abundant OTUs were identified, which represented >90 % of the total sequences. The most abundant sequences from each OTU were selected for taxonomic identification, using the massBLASTER implemented in PlutoF against the UNITE (Abarenkov et al., 2010). In addition, the taxonomic assignment was supported using PROTAX analysis with 50 % probability in the PlutoF platform (Abarenkov et al., 2018). Taxonomic identities at the species level were assigned using >98.5 % similarity. Functional identification was supported using FUNGuild (Nguyen et al., 2016) for descriptive assessment of the fungal communities, but analyses were based only on broad functional guilds (ECM and saprotrophic fungi). Since FUNGuild database presents

uncertainties on several fungal taxa, functional identification was also supported with other databases (Castaño et al., 2023; Clemmensen et al., 2021, 2015).

### 2.7. Statistical analyses

Statistical analyses were performed in the R software environment (v.2022.12.0; R Development Core Team, 2020), using the “vegan” package for multivariate and diversity analyses (Oksanen et al., 2018), and “nlme” package for linear and generalized mixed models (Pinheiro et al., 2013).

Soil fungal data were analyzed using both multivariate and univariate methods. Before any analyses, fungal data was Hellinger-transformed. Soil fungal compositional differences between the four tree species stands were tested using Permutational Multivariate Analysis of Variance (PMAV, ‘adonis’ function using Bray-Curtis distance). Here, an overall analysis was conducted stratified by depth, and after that, soil fungi data was split into two soil layers (top vs. bottom). We also used PMAV to test interactions between host and soil depth in community composition. Here, the spatial structure of the data was considered restricting the permutations to plots. Since similar results between hosts were obtained for both depths separately, we decided to not split the depths in the subsequent soil-community analyses. Nonmetric multidimensional scaling (NMDS, ‘metaMDS’ function with Bray–Curtis distance) was used to visualize the compositional differences between the forest stands. Afterward, the centroids of each forest habitat were overlaid in the ordination space (‘envfit’ function), with their standard deviational ellipses (‘ordiellipse’ function).

To identify associations between fungal compositional differences and soil parameters (pH, bulk density, total carbon, TOC, total N, total soluble N (TN<sub>b</sub>), ammonium, nitrate, DON, δ<sup>15</sup>N, C:N ratio, Olsen extractable P), variables were fit onto the overall NMDS ordination plot using the ‘envfit’ function and 999 permutations. In addition, using only the significant soil parameters, we fitted response surface models over

NMDS ordination results using general additive models (GAM) by ‘ordisurf’ function to identify the linearity of these trends.

Linear Mixed-Effects (LME) models were used to test significant changes in diversity (OTU richness and evenness calculated for each sample) between hosts and two soil layers. Here, we included square-root transformed read counts as explaining variable to account for variation in sequencing depth (Bálint et al., 2015). In the overall analysis, plot identity was defined as a random factor while the host was defined as fixed factor. The same LME scheme was followed to test relationships between the relative abundances of each fungal guild and the significant soil variables obtained from envfit function in the previous section.

## 3. Results

### 3.1. Soil parameters differ among forest stands

There were significant differences in soil characteristics among forest stands (Table 1). Soil pH at both soil depths (0–5 and 5–15 cm) were the highest in *R. pseudoacacia* ( $P < 0.01$ ) while pH values did not differ among the other forests. There were significant differences in soil C and N stocks among forest stands (Table 2). Total soil C stocks were the highest in *F. crenata* and the lowest in *L. kaempferi* forests ( $P < 0.05$ ). Total N was similar in all stands except for *L. kaempferi*, where it was the lowest ( $P < 0.05$ ). Total soluble N was highest in *C. japonica* and *F. crenata* and lowest in *L. kaempferi* and *R. pseudoacacia* stands ( $P < 0.05$ ). Dissolved organic N was the lowest in *F. crenata* and *R. pseudoacacia* and the highest in *C. japonica* (min.  $P < 0.05$ ). Ammonium was the lowest in *L. kaempferi* and *R. pseudoacacia* and the highest in *F. crenata* (min.  $P < 0.05$ ). Nitrate was the highest in *R. pseudoacacia* and *C. japonica* while almost negligible in the other forests (min.  $P < 0.05$ ).

Soil C:N ratio in *F. crenata* plots was higher than in the AM type *C. japonica* ( $P < 0.05$ ) and the bottom layer of *R. pseudoacacia* ( $P < 0.01$ )

**Table 1**

Soil characteristics of mineral soil under *Fagus crenata* ( $n = 9$ ), *Larix kaempferi* ( $n = 8$ ), *Cryptomeria japonica* ( $n = 9$ ), and *Robinia pseudoacacia* ( $n = 5$ ) with ± denoting SD. TOC represents total organic carbon and DON extractable dissolved organic nitrogen. pH, bulk density and Olsen extractable P were only determined in 3 samples per species. Capital letters indicate significant differences between tree species among the same soil depth and small letters indicate significant differences between soil depths among the same species ( $P > 0.05$ ).

Fungal association	Species	Depth	pH	Bulk density	total C	total N	C: N	TOC	total soluble N	NH <sub>4</sub> <sup>+</sup> -N	NO <sub>3</sub> <sup>-</sup> -N	DON	δ <sup>15</sup> N	Olsen extractable P
		cm		g cm <sup>-3</sup>	g kg <sup>-1</sup>	g kg <sup>-1</sup>		mg kg <sup>-1</sup>	mg kg <sup>-1</sup>	mg kg <sup>-1</sup>	mg kg <sup>-1</sup>	mg kg <sup>-1</sup>	‰	mg kg <sup>-1</sup>
Ecto-mycorrhizal	<i>Fagus crenata</i>	0–5	3.6 ± 0.1 <sup>B</sup>	0.8 ± 0.1	164.9 ± 64.8 <sup>Aa</sup>	8.5 ± 2.4 <sup>Aa</sup>	21.6 ± 2.9 <sup>A</sup>	500 ± 213 <sup>A</sup>	302 ± 73 <sup>ABa</sup>	253 ± 59 <sup>Aa</sup>	4 ± 6 <sup>B</sup>	39 ± 41 <sup>B</sup>	0.7 ± 1.7 <sup>b</sup>	35.8 ± 16.0 <sup>AB</sup>
		5–15	3.7 ± 0.3 <sup>B</sup>	0.9 ± 0.1 <sup>B</sup>	69.3 ± 6.0 <sup>Ab</sup>	4.1 ± 1.0 <sup>ACb</sup>	18.5 ± 5.3 <sup>A</sup>	318 ± 44 <sup>A</sup>	177 ± 30 <sup>Ab</sup>	149 ± 37 <sup>Ab</sup>	3 ± 4 <sup>B</sup>	41 ± 43 <sup>B</sup>	2.9 ± 1.8 <sup>a</sup>	20.8 ± 8.6 <sup>AB</sup>
	<i>Larix kaempferi</i>	0–5	4.1 ± 0.5 <sup>B</sup>	1.0 ± 0.2	41.1 ± 2.9 <sup>Ba</sup>	2.3 ± 0.1 <sup>Ba</sup>	18.2 ± 5.8 <sup>AB</sup>	174 ± 91 <sup>BC</sup>	138 ± 58 <sup>BC</sup>	8 ± 3 <sup>B</sup>	1 ± 1 <sup>B</sup>	129 ± 55 <sup>AB</sup>	0.9 ± 1.5	16.0 ± 8.5 <sup>AB</sup>
		5–15	4.3 ± 0.3 <sup>B</sup>	1.2 ± 0.2 <sup>A</sup>	30.1 ± 3.1 <sup>Cb</sup>	1.8 ± < 0.1 <sup>Bb</sup>	16.5 ± 4.1 <sup>AB</sup>	106 ± 30 <sup>C</sup>	88 ± 8 <sup>B</sup>	5 ± 1 <sup>C</sup>	1 ± < 1 <sup>B</sup>	82 ± 8 <sup>AB</sup>	2.0 ± 1.5	10.0 ± 5.0 <sup>B</sup>
Arbuscular mycorrhizal	<i>Cryptomeria japonica</i>	0–5	4.4 ± 0.4 <sup>B</sup>	0.8 ± 0.1	96.9 ± 29.7 <sup>ABa</sup>	6.7 ± 1.2 <sup>Aa</sup>	14.2 ± 3.5 <sup>B</sup>	470 ± 100 <sup>ABa</sup>	390 ± 111 <sup>Aa</sup>	139 ± 126 <sup>ABa</sup>	20 ± 24 <sup>Ba</sup>	230 ± 98 <sup>A</sup>	0.8 ± 1.3	41.3 ± 20.9 <sup>A</sup>
		5–15	4.6 ± 0.1 <sup>B</sup>	0.9 ± 0.1 <sup>B</sup>	77.0 ± 12.7 <sup>Ab</sup>	5.5 ± 1.0 <sup>Ab</sup>	14.5 ± 2.9 <sup>B</sup>	208 ± 38 <sup>Bb</sup>	208 ± 42 <sup>Ab</sup>	35 ± 46 <sup>BCb</sup>	10 ± 13 <sup>ABb</sup>	163 ± 62 <sup>A</sup>	2.9 ± 1.2 <sup>b</sup>	21.5 ± 16.3 <sup>AB</sup>
	<i>Robinia pseudoacacia</i>	0–5	5.6 ± 0.1 <sup>Aa</sup>	0.8 ± 0.1 <sup>b</sup>	126.6 ± 34.7 <sup>ABa</sup>	7.4 ± 1.7 <sup>Aa</sup>	22.6 ± 6.6 <sup>Aa</sup>	145 ± 6 <sup>BCa</sup>	143 ± 7 <sup>Ba</sup>	12 ± 1 <sup>Ba</sup>	50 ± 6 <sup>Aa</sup>	83 ± 3 <sup>AB</sup>	0.5 ± 0.9	34.0 ± 5.2 <sup>AB</sup>
		5–15	5.4 ± 0.1 <sup>Ab</sup>	1.1 ± 0.1 <sup>ABa</sup>	36.9 ± 13.6 <sup>BCb</sup>	2.9 ± 0.8 <sup>BCb</sup>	11.1 ± 3.2 <sup>Bb</sup>	64 ± 5 <sup>Cb</sup>	100 ± 1 <sup>Bb</sup>	5 ± < 1 <sup>Cb</sup>	19 ± < 1 <sup>Ab</sup>	77 ± 5 <sup>AB</sup>	2.2 ± 0.6	12.6 ± 6.0 <sup>AB</sup>

**Table 2**

Soil nutrient stocks, weighted mean pH and  $\delta^{15}\text{N}$  in the first 15 cm of mineral soil ( $\pm$  SD) under *Fagus crenata*, *Larix kaempferi*, *Cryptomeria japonica*, and *Robinia pseudoacacia* with  $\pm$  denoting SD ( $n = 3$  per species). Letters indicate significant differences between species (lme anova,  $P < 0.05$ ). DON represents extracted dissolved organic nitrogen.

Fungal association	Species	pH	total C kg m <sup>-2</sup>	total N kg m <sup>-2</sup>	total soluble N g m <sup>-2</sup>	NH <sub>4</sub> <sup>+</sup> -N g m <sup>-2</sup>	NO <sub>3</sub> <sup>-</sup> -N g m <sup>-2</sup>	DON g m <sup>-2</sup>
Ecto-mycorrhizal	<i>Fagus crenata</i>	3.6 $\pm$ 0.2 <sup>b</sup>	11.7 $\pm$ 3.1 <sup>a</sup>	0.8 $\pm$ 0.2 <sup>a</sup>	28.1 $\pm$ 5.9 <sup>a</sup>	23.8 $\pm$ 7.0 <sup>a</sup>	0.4 $\pm$ 0.5 <sup>b</sup>	4.9 $\pm$ 4.5 <sup>b</sup>
	<i>Larix kaempferi</i>	4.2 $\pm$ 0.4 <sup>b</sup>	4.7 $\pm$ 0.4 <sup>b</sup>	0.4 $\pm$ <0.1 <sup>b</sup>	17.4 $\pm$ 0.7 <sup>b</sup>	1.0 $\pm$ 0.1 <sup>b</sup>	0.2 $\pm$ 0.2 <sup>b</sup>	16.2 $\pm$ 0.7 <sup>ab</sup>
Arbuscular mycorrhizal	<i>Cryptomeria japonica</i>	4.3 $\pm$ 0.5 <sup>b</sup>	7.8 $\pm$ 1.7 <sup>ab</sup>	0.8 $\pm$ 0.2 <sup>a</sup>	35.0 $\pm$ 3.3 <sup>a</sup>	8.6 $\pm$ 6.2 <sup>b</sup>	1.7 $\pm$ 2.1 <sup>ab</sup>	24.6 $\pm$ 10.5 <sup>a</sup>
	<i>Robinia pseudoacacia</i>	5.4 $\pm$ 0.1 <sup>a</sup>	9.5 $\pm$ 0.8 <sup>a</sup>	0.7 $\pm$ 0.3 <sup>ab</sup>	16.6 $\pm$ 0.4 <sup>b</sup>	1.0 $\pm$ 0.1 <sup>b</sup>	4.1 $\pm$ 0.2 <sup>a</sup>	11.7 $\pm$ 0.1 <sup>ab</sup>

(Table 1), while the ECM type *L. kaempferi* showed a similar soil C:N ratio compared to all forest types. When inspecting deep-wise changes in soil C:N ratios, these were only significantly different and decreased in *R. pseudoacacia* stands ( $P < 0.01$ ). Soil  $\delta^{15}\text{N}$  nor Olsen extractable P differed noteworthy among species.

### 3.2. Soil fungal communities

A total of 690,248 out of 1,526,648 sequences (45 %) passed quality

filtering. Single-linkage clustering resulted in 3111 OTUs, of which 600 (93 % of the high-quality sequences) were assessed for identification to species level and functional guild. We obtained an average of 10,774 reads per sample. This corresponded to 172,562 reads per plot (69,024 reads per stand). Overall, Ascomycota dominated the fungal community (57 % of the identified sequences), followed by Basidiomycota (22 %), others (5 %) and unknown (16 %). Ascomycota was represented by Letiomycetes (31 %), Sordariomycetes (17 %), Eurotiomycetes (10 %) and Dothiedomycetes (8 %). Also, 12 % of the remaining reads were

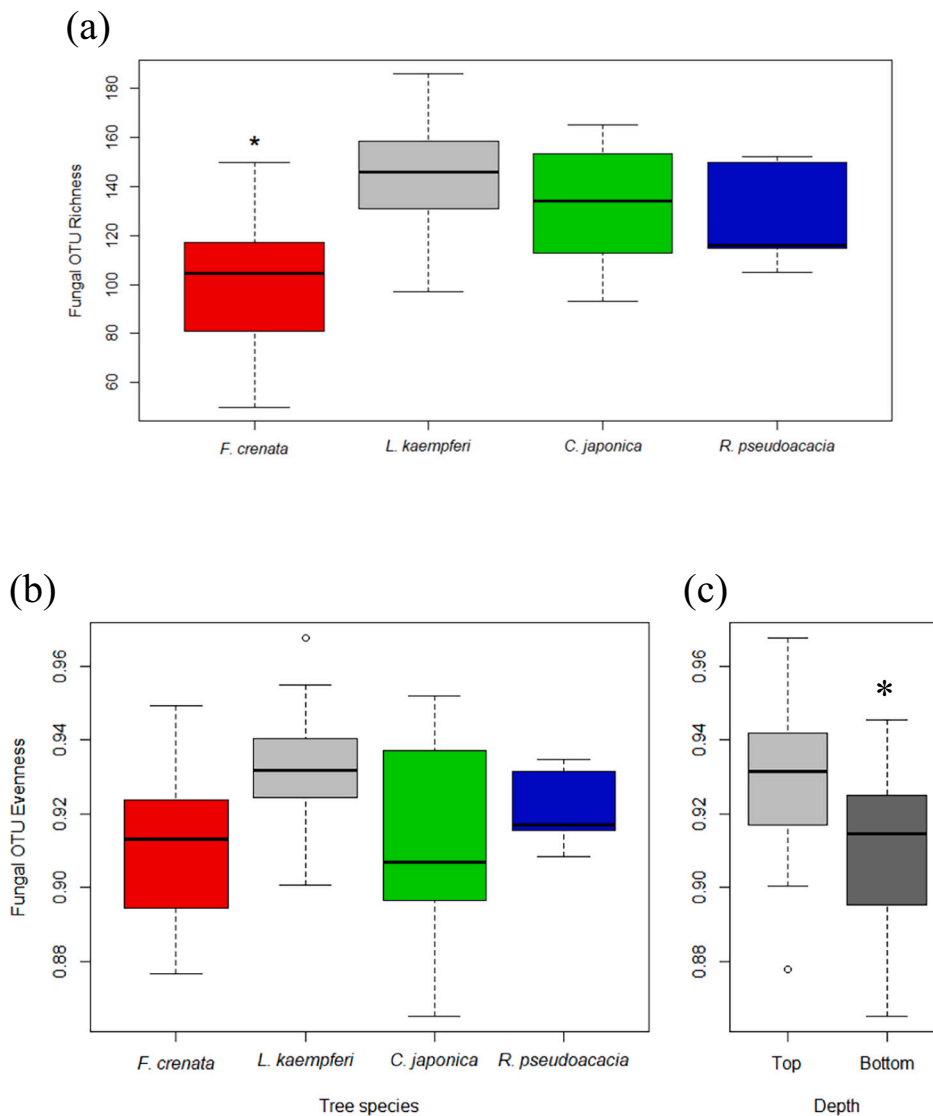


**Fig. 2.** Differences in fungal species richness (a), evenness (b) and evenness with soil depth (0–5 cm and 5–15 cm) (c) of *Fagus crenata*, *Larix kaempferi*, *Cryptomeria japonica*, and *Robinia pseudoacacia*. There was no significant difference in richness between soil depths. Asterisks indicate significant differences between habitats and depths ( $P < 0.01$ ).

represented by up to 18 different classes while 22 % remained unknown. Among Basidiomycota, 86 % belonged to Agaricomycetes and 7 % to seven other classes while another 7 % remained unknown. Overall, the ECM community was dominated by fungi with short-medium smooth-contact exploration types such as *Cenococcum*, *Lactarius*, *Russula*, *Lactifluus*, while long and medium fringe types were almost non-existent. *Mortierella* (mold) was the most abundant genera in the whole dataset.

### 3.3. Patterns in soil fungal communities across forest stands and soil layers

There were significant differences in soil fungal richness between forest stands ( $P = 0.010$ ), mainly driven by *F. crenata* stands that showed a significantly lower richness ( $107 \pm 15$ ) than all the other forest stands plots (Fig. 2a). No differences in fungal richness were found for soil depth ( $P > 0.05$ ). Further, there were no differences in species evenness ( $P > 0.05$ ) suggesting that fungal composition was evenly distributed between hosts. In addition, there were no differences in richness nor evenness between AM and ECM species ( $P > 0.05$ ). Simultaneously, evenness values were higher than 0.9 for all stands indicating that there was no species dominance among the fungal communities (Fig. 2b). However, the upper soil layer showed significantly greater evenness ( $P < 0.01$ ) than the deeper (Fig. 2c). In addition, we found a lower beta diversity of fungi in *F. crenata* plots (Fig. S1).

Forest habitat had a significant effect on soil fungal composition (PMAV all data: 999 permutations;  $P < 0.001$ ) and accounted for 46 % of the variance in the species data (Fig. 3). When the fungal dataset was split in the two soil depths, we observed the same significant patterns between host in each layer independently (PMAV top and bottom data: 999 permutations;  $P < 0.001$ ). However, when considering the soil depth in the analyses, we observed a significant effect of forest habitat x depth interaction on soil fungal composition explaining 4 % of the variance (PMAV all data: 999 permutations;  $P < 0.001$ ). The habitat x depth interaction was caused by the lack of differences in fungal composition between the top and bottom layers of *C. japonica* host ( $P > 0.05$ ), while fungal communities in the other hosts changed with depth.

The NMDS ordination (stress 0.12) showed that the overall distribution of plots reflected the differences among forest stands (Fig. 3). The ordination plot significantly separated the four tree species stands along the two ordination axes; with *F. crenata* located at the positive end of the

nm1 axis, *L. kaempferi* in a central position, and both *C. japonica* and *R. pseudoacacia* at the negative end of the X-axis. Simultaneously, *C. japonica* and *R. pseudoacacia* were significantly separated along the nm2 axis (Fig. 3). There were also fungal functional differences across the four tree species stands. ECM fungi were the most abundant in *F. crenata* and *L. kaempferi* ( $P < 0.01$ ), while they were almost absent in *R. pseudoacacia* and *C. japonica* (Fig. 4). Saprotrophs but also plant pathogens were the most abundant fungal group in *R. pseudoacacia* ( $P < 0.01$ ) followed by *C. japonica* and *L. kaempferi* and *F. crenata* ( $P < 0.05$ , Fig. 4).

### 3.4. Correlation between fungal communities and soil parameters

From the set of soil environmental parameters (Table 1) only 3 variables namely nitrate, C:N ratios and pH, explained a significant proportion of the variance in fungal community composition (all three accounting for 35 %,  $P < 0.05$ ; Fig. 5a). In general, pH (Fig. 5b) and nitrate (Fig. 5c) isolines increased almost linearly towards the negative ends of nm1 and nm2 in the ordination plots, towards *R. pseudoacacia* and *C. japonica* plots, typically dominated by fungal saprotrophs, while the inverse pattern was observed for C:N (Fig. 5d). In detail, pH was positively correlated with abundances of saprotrophic fungi ( $P < 0.05$ , Fig. 5a) and negatively with ECM fungi, particularly in the 5–15 cm soil layer ( $P < 0.01$ , Fig. 6a). For nitrate, we found a significant negative relationship with ECM fungi ( $P < 0.05$ , Fig. 6b) but no significant relationship with the relative abundances of saprotrophs ( $P > 0.05$ , Fig. 5c). Further, C:N ratios isolines were non-linearly increasing towards the positive nm1 and nm2 axes, near *L. kaempferi* and *F. crenata* stands (Fig. 5d), which were dominated by ECM fungi. Positive associations were found between C:N ratios and ECM fungi ( $P < 0.05$  for both horizons, Fig. 6c), but also root-associated fungi ( $P < 0.05$  for both horizons, Fig. 6d). No associations were found between ammonium content and abundance of any of the fungal guilds ( $P > 0.050$ ) as well as between C and N content with any of the fungal guilds ( $P > 0.050$ ).

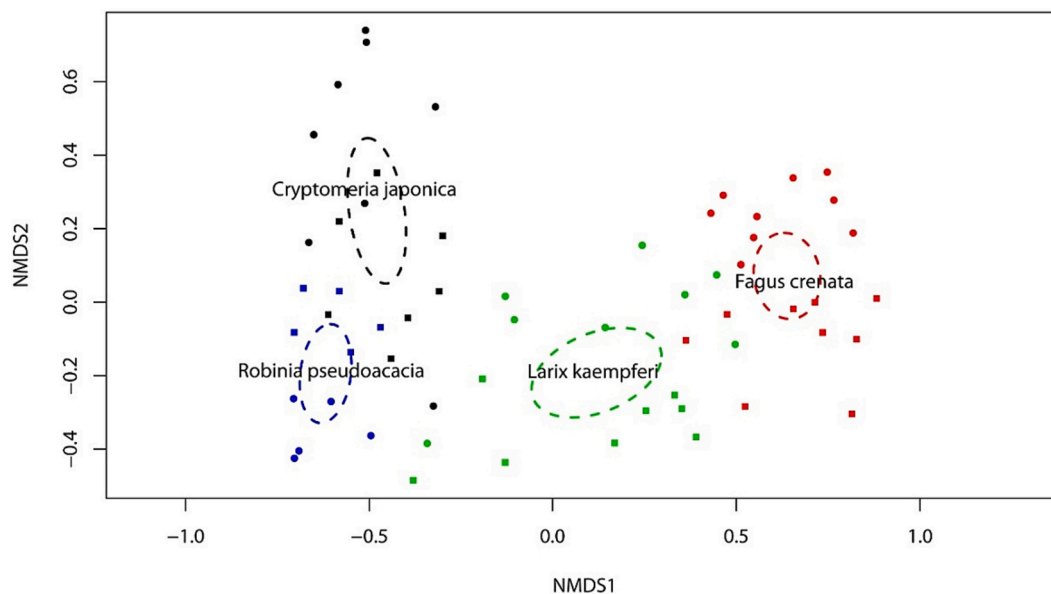


Fig. 3. NMDS plot of fungal composition in *Fagus crenata*, *Larix kaempferi*, *Cryptomeria japonica*, and *Robinia pseudoacacia*. The host SD-ellipses indicated that the four host were in different regions of the ordination space.

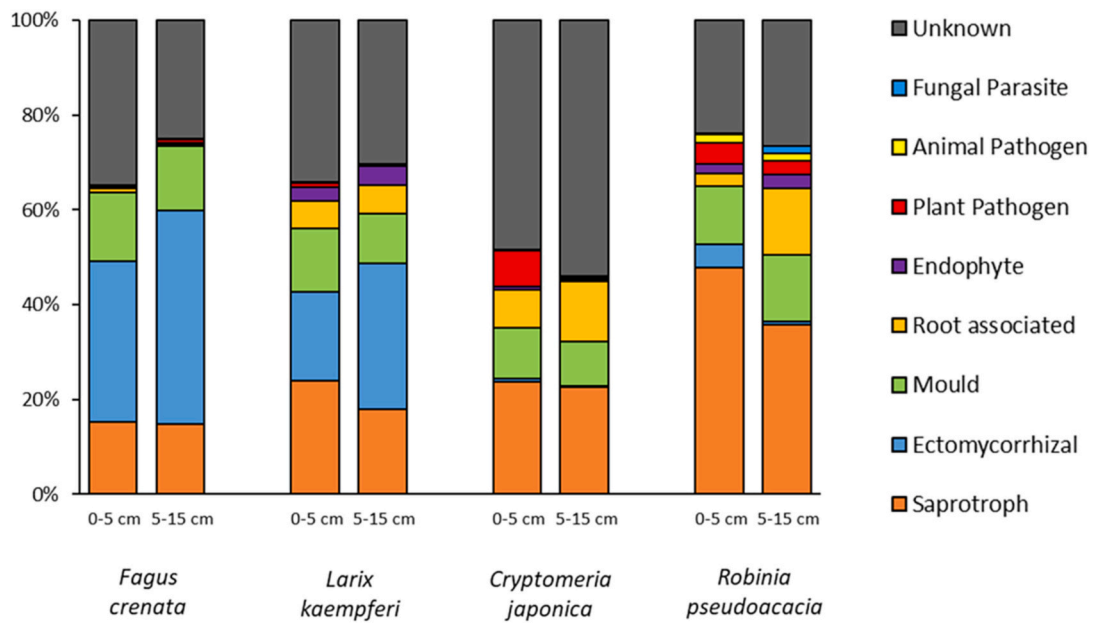


Fig. 4. Fungal community structure of *Fagus crenata*, *Larix kaempferi*, *Cryptomeria japonica*, and *Robinia pseudoacacia* (n = 9, 8, 9 and 5 per species respectively) in two different soil depths (0–5 cm. and 5–15 cm.)

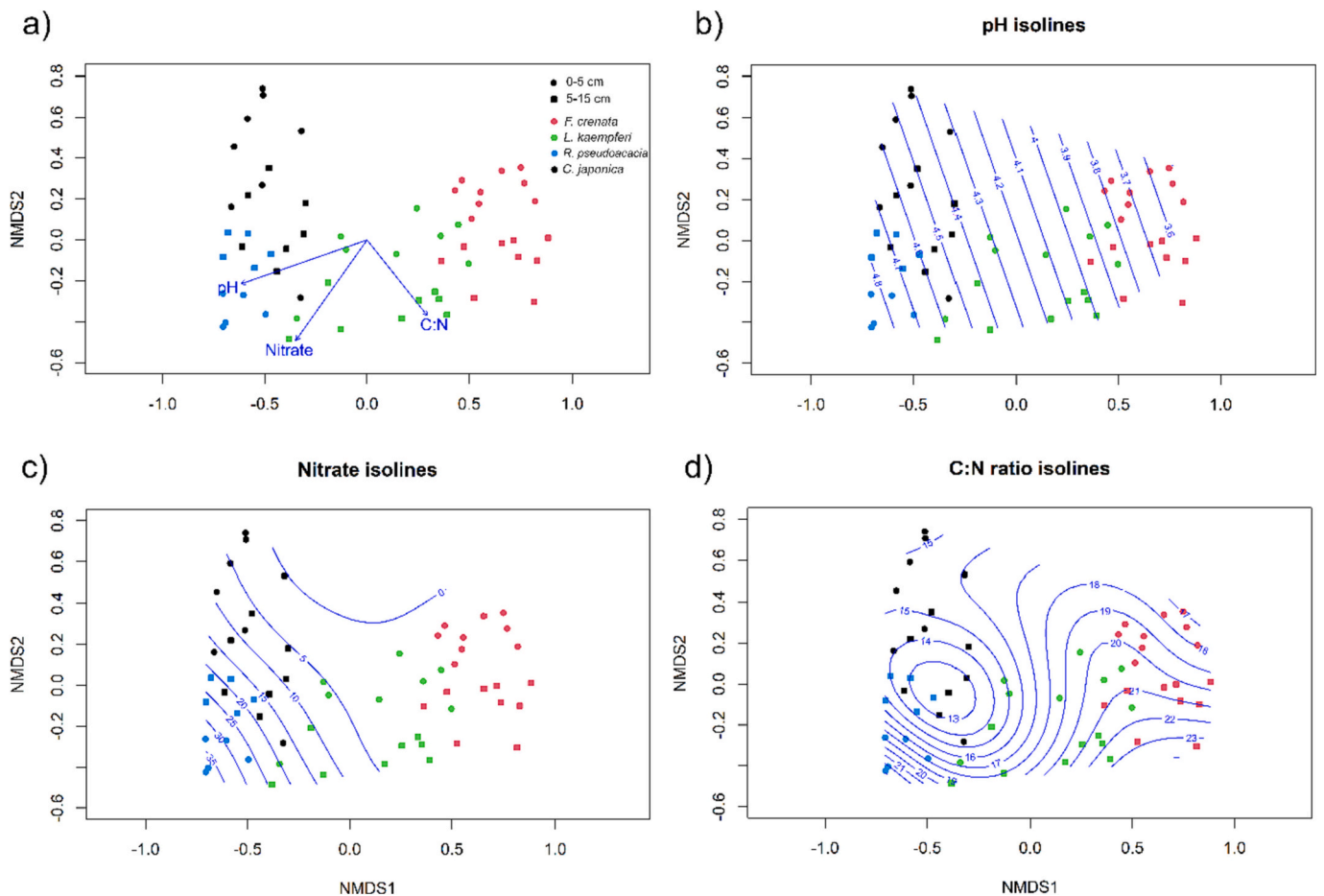


Fig. 5. Correlation of fungal community structure with soil parameters (a), pH (b), nitrate content (c) and C/N ratio (d) of *Fagus crenata*, *Larix kaempferi* (both species associated with ectomycorrhizal colonization), *Cryptomeria japonica*, and *Robinia pseudoacacia* (both species associated with arbuscular mycorrhizal colonization).

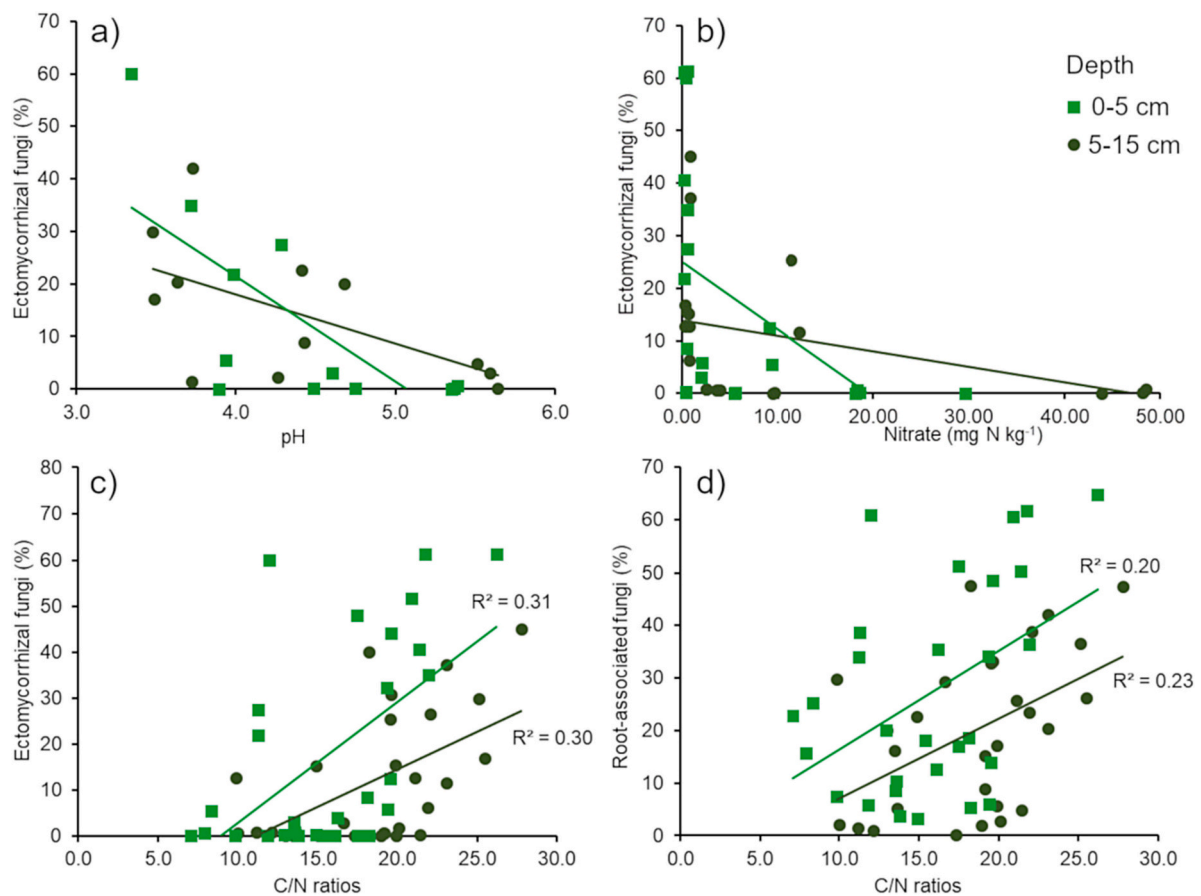


Fig. 6. Associations between the abundance of ECM fungi and pH (a), and Nitrate (b). Associations between soil C/N ratios and the abundance of ECM fungi (c) or root-associated fungi (d). In each of the panels the two topsoil depths are shown in green (0–5 cm) and in brown (5–15 cm) colour.

## 4. Discussion

### 4.1. Patterns in fungal communities among forest stands and soil layers

In agreement with our first hypothesis, we found strong fungal compositional and functional differences among the four forest stands. However, fungal evenness and richness values were similar across all stands except for *F. crenata*, which showed the lowest richness.

As expected, *L. kaempferi* and *F. crenata* showed a higher abundance of ECM taxa while these were lacking in *R. pseudoacacia* and *C. japonica*, which were more dominated by fungal saprotrophs. Dominance by fungal saprotrophs in AM types has been previously shown (Cheeke et al., 2017; Phillips et al., 2013) and has been linked to enhanced soil organic matter decomposition (Averill et al., 2014; Steidinger et al., 2019). Interestingly, many fungal taxonomies and functions in *C. japonica* stands were unknown, which stresses the importance of gaining better knowledge on the fungal communities inhabiting this species as it is the most important commercial tree species in Japan (Seidel et al., 2019a).

Molds were particularly abundant in all forest stands, potentially promoted by the very wet conditions of the plots (Hartmann et al., 2017; Santalahti et al., 2016). Similarly, across all forest stands the ECM community was mainly dominated by fungal taxa with simple mycelia (e. g. medium smooth, contact, short exploration types), such as *Russula*, *Cenococcum*, *Lactarius*, and *Lactifluus*. Particularly *Lactarius* spp. was also observed to be dominant in cool-temperate subalpine Japanese forests (Shigyo et al., 2019). By contrast, fungal species with nitrophobic mycelia such as *Suillus* spp., *Rhizopogon* spp., or *Piloderma* spp. (Almeida et al., 2022; Lilleskov et al., 2002) or species such as *Cortinarius* or *Boletus* that can mine N from organic substrates (Lindahl and Tunlid,

2015), were absent. Potentially, the overall dominance of saprotrophs such as molds in the system suggests fast organic matter turnover and relatively higher N availability than other cold ecosystems. It seems that ECM fungi might be dominating *F. crenata* soils, provided by the lowest fungal richness and evenness but high levels of ECM fungi. Potentially, these mycorrhizal fungi may be monopolizing nutrients and competing with saprotrophs (Näsholm et al., 2013). By contrast, we detected very low abundance of AM species, potentially because the high abundance of other fungi such as saprotrophs overshadow the presence of arbuscular mycorrhizal fungi in these systems.

### 4.2. Patterns of main soil chemical variables and fungal communities

It is well known that pH strongly affects fungal communities and fungal growth (Adamo et al., 2021a; Qiang et al., 2021; Rousk et al., 2009, 2010) as observed in our study. Lower pH values result in increasing phylogenetic community similarity of ECM species (Adamo et al., 2021b), which could further support the lower beta diversity of fungi observed in our *F. crenata* plots (Fig. S1). By contrast, our results showed that greater pH values were more related to saprotroph abundances in *R. pseudoacacia* and *C. japonica* hosts, which were also related to higher soil nitrates. Fungal saprotrophs are known to have a strong influence on decomposition processes by decomposing OM and releasing inorganic N during the process (Phillips et al., 2013), but potentially bacterial nitrifiers could be very important in this system as well.

Depth-wise variation in C:N was only observed in *R. pseudoacacia*. These lack of differences with soil depth may be because we did not include the litter layer, which is often monopolized by fungal saprotrophs and thus has different fungal communities than more mineral soil

layers (Andreetta et al., 2011; Jumpponen et al., 2010; Voříšková et al., 2014). However, in our study the litter layer was thin in all plots except for *F. crenata*, potentially indicating efficient degradation of fresh litter. Besides the different depth-wise C:N patterns in *R. pseudoacacia*, patterns in soil C:N ratios among mycorrhizal types did not fully match our second hypothesis, although *C. japonica* had lower C:N values than *F. sylvatica*. It is expected that soil C:N ratios are higher in ECM types compared to AM types (Averill et al., 2014; Zhu et al., 2018) due to enhanced decomposition processes in the latter type. In our case, soil C:N ratios of *L. kaempferi* did not differ from the other forests, potentially because both soil C and N were low.

For both soil layers, soil C:N ratios correlated with the relative abundances of ECM fungi across all samples. C:N or depth-wise patterns in soil C:N ratios have been shown to indicate the strength of saprotrophic processes (Fernandez et al., 2019), inhibition of decomposition processes (Averill, 2016) and mycorrhizal-driven N mining (Clemmensen et al., 2013, 2015). Thus, soil C:N ratios may reflect the pathway by which N is recycled (Averill et al., 2014). The links between C:N ratios and the abundances of root-associated fungi suggest that root-associated fungi promote shifts towards organic N cycling (Castaño et al., 2023; Grau et al., 2019; Phillips et al., 2013) and that these fungi are important drivers of C:N ratios in topsoils, in addition to litter quality inputs (Wurzburger and Hendrick, 2009). Concerning these inputs, plant and microbial litter quality and thus C:N ratios can also vary between vegetation types and thus affect soil parameters (Robinson et al., 2020; Wurzburger and Hendrick, 2009). For example, it has been suggested that AM types have higher litter quality, which enhances denitrification processes and inorganic N cycling, while low quality litter of ECM vegetation types promote ECM species able to decompose more recalcitrant organic matter fractions (Phillips et al., 2013; Hedéneć et al., 2020). Although in our study we did not assess C:N ratios in litter, generally conifers have higher C:N ratios than deciduous trees (Zhang et al., 2020). However, these differences in litter C:N ratios potentially did not match that of soils, since we observed a tendency for the deciduous tree *Fagus sylvatica* to have higher soil C:N ratios. Our results also support recent findings showing tight links between organic nutrient economy and the abundance of ectomycorrhizal species (Hedéneć et al., 2023), however, among contrasting mycorrhizal types inorganic N cycling dominating AM types was mainly supported by the high inorganic N in these types rather than low C:N ratios. We observed higher ammonium content in *C. japonica* plots, while nitrate was higher in *R. pseudoacacia*, indicating that dominating mechanisms for N cycling were distinct between both AM types. *R. pseudoacacia* can cover up to 76 % of its high N demand by uptaking N from the atmosphere via Frankia nodules (Marron et al., 2018; Seidel et al., 2022). Potential soil N availability was the lowest in *L. kaempferi* forests, where ammonium and nitrate levels were very low. The unexpected high ammonium content in *F. crenata* could be by N retention of highly abundant ECM taxa (Näsholm et al., 2013) but this remains to be tested.

#### 4.3. Links between soil C and N stocks and soil fungal communities

Although differences in C and N stocks were found among tree species, these were not consistent within mycorrhizal types, rejecting our third hypothesis. However, *L. kaempferi* plots had the lowest soil C and N stocks, compared to the other stands. A possibility would be that ECM-driven decomposition processes were only occurring in *L. kaempferi*, potentially due to the lower N availability in this forest compared to *F. crenata*. However, we did not observe potential mycorrhizal oxidizers that could promote organic matter decomposition (Lindahl and Tunlid, 2015), since most of the observed ECM taxa in the whole dataset had simple exploration types of mycelia (i.e. contact, medium smooth, or short types). Seidel et al. (2019a, 2019b, 2022) previously showed that litter production was highest in *F. crenata*, followed by *C. japonica*, *R. pseudoacacia* and *L. kaempferi* ( $8.7 \pm 0.2^a$ ,  $6.9 \pm 0.9^b$ ,  $4.8 \pm 0.9^c$ ,  $4.0 \pm 0.8^c$  kg per m<sup>2</sup> Litter respectively). Since above-ground litter barely

interact with soil minerals and other root-derived compounds, the long-term stability of litter-derived organic matter is assumed to be low (Cotrufo et al., 2013). However, litter additions, particularly that of high quality, can promote activities of microorganisms, particularly fungi (Liang et al., 2017; Wei et al., 2022). Higher microbial activities and particularly microbial residues can in turn contribute to soil organic matter accumulation (Cotrufo et al., 2013) if these interact with soil minerals (i. e. entombing effect (Liang et al., 2017)). We speculate that this could be the case for *F. crenata* and *C. japonica* and that litter and microbial residues could be stabilized faster in these forests with higher litter production. However, the relevance of this mechanism for C stabilization in this particular system would need to be further tested.

## 5. Conclusion

In this study, we investigated the fungal communities in soils from different forest stands dominated by four widespread Japanese tree species of the cold-temperate zone. Soil fungal communities differed among forest stands and were related to soil pH, nitrate content, and C:N ratios. Distinct nutrient cycling economy was observed among the four forest species but indicators for nutrient economy among mycorrhizal types (AM vs ECM) were not consistent. The observed links between soil characteristics (C:N ratios, ammonium, and nitrate) and the relative abundances of root-associated fungi and saprotrophs stress the importance of these guilds for influencing nutrient cycling economy across contrasting vegetation types. The disparate C stocks observed between *L. kaempferi* and *F. crenata* suggest distinct below or above-ground processes influencing element stocks.

Supplementary data to this article can be found online at <https://doi.org/10.1016/j.apsoil.2024.105360>.

### CRedit authorship contribution statement

**Felix Seidel:** Conceptualization, Data curation, Formal analysis, Investigation, Methodology, Software, Validation, Visualization, Writing – original draft, Writing – review & editing. **Carles Castaño:** Conceptualization, Formal analysis, Methodology, Software, Validation, Visualization, Writing – review & editing. **Josú G. Alday:** Data curation, Formal analysis, Methodology, Software, Validation, Visualization, Writing – review & editing. **M. Larry Lopez C.:** Conceptualization, Supervision, Writing – review & editing. **José Antonio Bonet:** Conceptualization, Resources, Supervision, Writing – review & editing.

### Declaration of competing interest

The authors declare that they have no known competing financial interests or personal relationships that could have appeared to influence the work reported in this paper.

### Data availability

All data of this study is found in a Zenodo repository: <https://doi.org/10.5281/zenodo.7848882>

Data on the sequencing will be uploaded in the next manuscript version in NCBI (<https://www.ncbi.nlm.nih.gov/>).

### Acknowledgements

We want to thank the staff of the University Research Forest of Yamagata University for keeping the forest accessible in summer and winter.

### References

- Abarenkov, K., Nilsson, R.H., Larsson, K.-H., Alexander, I.J., Eberhardt, U., Erland, S., Høiland, K., Kjoller, R., Larsson, E., Pennanen, T., Sen, R., Taylor, A.F.S.,

- Tederso, L., Ursing, B.M., Vrålstad, T., Liimatainen, K., Peintner, U., Kõljalg, U., 2010. The UNITE database for molecular identification of fungi – recent updates and future perspectives. *New Phytol.* 186, 281–285.
- Abarenkov, K., Somervuo, P., Nilsson, R.H., Kirk, P.M., Huotari, T., Abrego, N., Ovaskainen, O., 2018. Protax-fungi: a web-based tool for probabilistic taxonomic placement of fungal internal transcribed spacer sequences. *New Phytol.* 220 (2), 517–525. <https://doi.org/10.1111/nph.15301>.
- Adamo, I., Castaño, C., Bonet, J.A., Colinas, C., Martínez de Aragón, J., Alday, J.G., 2021a. Soil physico-chemical properties have a greater effect on soil fungi than host species in Mediterranean pure and mixed pine forests. *Soil Biol. Biochem.* 160 (2021), 108320 <https://doi.org/10.1016/j.soilbio.2021.108320>.
- Adamo, I., Castaño, C., Bonet, J.A., Colinas, C., Martínez de Aragón, J., Alday, J.G., 2021b. Lack of phylogenetic differences in ectomycorrhizal fungi among distinct Mediterranean pine forest habitats. *J. Fungi* 7, 793. <https://doi.org/10.3390/jof7100793>.
- Almeida, J.P., Rosenstock, N.P., Woche, S.K., Guggenberger, G., Wallander, H., 2022. Nitrophobic ectomycorrhizal fungi are associated with enhanced hydrophobicity of soil organic matter in a Norway spruce forest. *Biogeosciences* 19, 3713–3726. <https://doi.org/10.5194/bg-19-3713-2022>.
- Al-Shammary, A.A.G., Kouzani, A.Z., Kaynak, A., Khoo, S.Y., Norton, M., Gates, W., 2018. Soil bulk density estimation methods: a review. *Pedosphere* 28 (4), 581–596. [https://doi.org/10.1016/S1002-0160\(18\)60034-7](https://doi.org/10.1016/S1002-0160(18)60034-7).
- An, G.-H., Miyakawa, S., Kawahara, A., Osaki, M., Ezawa, T., 2008. Community structure of arbuscular mycorrhizal fungi associated with pioneer grass species *Miscanthus sinensis* in acid sulfate soils: habitat segregation along pH gradients. *Soil Sci. Plant Nutr.* 54, 517–528.
- Andreatta, A., Macci, C., Ceccherini, M.T., Cecchini, G., Masciandaro, G., Pietramellara, G., Carnicelli, S., 2011. Microbial dynamics in Mediterranean Moder humus. *Biol. Fertil. Soils* 48, 259–270.
- Averill, C., 2016. Slowed decomposition in ectomycorrhizal ecosystems is independent of plant chemistry. *Soil Biol. Biochem.* 102, 52–54. <https://doi.org/10.1016/j.soilbio.2016.08.003>.
- Averill, C., Turner, B.L., Finzi, A.C., 2014. Mycorrhiza-mediated competition between plants and decomposers drives soil carbon storage. *Nature* 505, 543–545. <https://doi.org/10.1038/nature12901>.
- Baldrian, P., Vorfisková, J., Dobiášová, P., Merhautová, V., Lisá, L., Valášková, V., 2011. Production of extracellular enzymes and degradation of biopolymers by saprotrophic microfungi from the upper layers of forest soil. *Plant Soil* 338, 111–125.
- Bálint, M., Bartha, L., O'hara, R.B., Olson, M.S., Otte, J., Pfenninger, M., Robertson, A.L., Tiffin, P., Schmitt, I., 2015. Relocation, high-latitude warming and host genetic identity shape the foliar fungal microbiome of poplars. *Mol. Ecol.* 24, 235–248.
- Cairney, J.W.G., 2012. Extramatrical mycelia of ectomycorrhizal fungi as moderators of carbon dynamics in forest soil. *Soil Biol. Biochem.* 47, 198–208.
- Castaño, C., Berlin, A., Brandström-Durling, M., Ihrmark, K., Lindahl, B.D., Stenlid, J., Clemmensen, K.E., Olson, Å., 2020. Optimized metabarcoding with Pacific biosciences enables semi-quantitative analysis of fungal communities. *New Phytol.* 228, 1149–1158. <https://doi.org/10.1111/nph.16731>.
- Castaño, C., Hallin, S., Egelkraut, D., Lindahl, B.D., Olofsson, J., Clemmensen, K.E., 2023. Contrasting plant-soil-microbial feedbacks stabilize vegetation types and uncouple topsoil C and N stocks across a subarctic-alpine landscape. *New Phytol.* 238 (6), 2621–2633. <https://doi.org/10.1111/nph.18679>.
- Cheeke, T.E., Phillips, R.P., Brzostek, E.R., Rosling, A., Bever, J.D., Fransson, P., 2017. Dominant mycorrhizal association of trees alters carbon and nutrient cycling by selecting for microbial groups with distinct enzyme function. *New Phytol.* 214, 432–442.
- Clemmensen, K.E., Bahr, A., Ovaskainen, O., Dahlberg, A., Ekblad, A., Wallander, H., Stenlid, J., Finlay, R.D., Wardle, D.A., Lindahl, B.D., 2013. Roots and associated fungi drive long-term carbon sequestration in boreal forest. *Science* 339, 1615–1618.
- Clemmensen, K.E., Finlay, R.D., Dahlberg, A., Stenlid, J., Wardle, D.A., Lindahl, B.D., 2015. Carbon sequestration is related to mycorrhizal fungal community shifts during long-term succession in boreal forests. *New Phytol.* 205, 1525–1536.
- Clemmensen, K.E., Brandström-Durling, M.B., Michelsen, A., Hallin, S., Finlay, R.D., Lindahl, B.D., 2021. A tipping-point in carbon storage when forest expands into tundra is related to mycorrhizal recycling of nitrogen. *Ecol. Lett.* 24, 1193–1204. <https://doi.org/10.1111/ele.13735>.
- Cotrufo, M.F., Wallenstein, M.D., Boot, C.M., et al., 2013. The Microbial Efficiency-Matrix Stabilization (MEMS) framework integrates plant litter decomposition with soil organic matter stabilization: do labile plant inputs form stable soil organic matter? *Glob. Chang. Biol.* 19, 988–995. <https://doi.org/10.1111/GCB.12113>.
- Crooke, W.M., Simpson, W.E., 1971. Determination of ammonium in Kjeldahl digest of crops by an automated procedure. *J. Sci. Food Agric.* 22, 9–10.
- DeBellis, T., Kernaghan, G., Widden, P., 2007. Plant community influences on soil microfungi assemblages in boreal mixed-wood forests. *Mycologia* 99, 356–367.
- Dighton, J., 2003. *Fungi in Ecosystem Process*. Marcel Dekker Inc, New Jersey.
- Edgar, R.C., 2010. Search and clustering methods of magnitude faster than BLAST. *Bioinformatics* 26, 2460–2461.
- Enta, A., Hayashi, M., Lopez Caceres, M.L., et al., 2020. Nitrogen resorption and fractionation during leaf senescence in typical tree species in Japan. *J. For. Res.* 31, 2053–2062. <https://doi.org/10.1007/s11676-019-01055-z>.
- FAO, 2006. *Guidelines for Soil Description*, 4th edition. FAO, ROME.
- Fernandez, C.W., Kennedy, P.G., 2016. Revisiting the 'Gadgil effect': do interguild fungal interactions control carbon cycling in forest soils? *New Phytol.* 209, 1382–1394. <https://doi.org/10.1111/nph.13648>.
- Fernandez, C.W., See, C.R., Kennedy, P.G., 2019. Decelerated carbon cycling by ectomycorrhizal fungi is controlled by substrate quality and community composition. *New Phytol.* 226, 569–582. <https://doi.org/10.1111/nph.16269>.
- Frey, B., Walthert, L., Perez-Mon, C., Stierli, B., Köchli, R., Dharmarajah, A., Brunner, I., 2021. Deep soil layers of drought-exposed Forests Harbor poorly known bacterial and fungal communities. *Front. Microbiol.* 12, 674160 <https://doi.org/10.3389/fmicb.2021.674160>.
- Fukasawa, Y., Osono, T., Takeda, H., 2009. Microfungus communities of Japanese beech logs at different stages of decay in a cool temperate deciduous forest. *Can. J. For. Res.* 39, 1606–1614.
- Grau, O., Saravesi, K., Ninot, J.M., Geml, J., Markkola, A., Ahonen, S.H.K., Peñuelas, J., 2019. Encroachment of shrubs into subalpine grasslands in the Pyrenees modifies the structure of soil fungal communities and soil properties. *FEMS Microbiol. Ecol.* 95, fiz028. <https://doi.org/10.1093/femsec/fiz028>.
- Hagenbo, A., Alday, J.G., Martínez de Aragón, J., Castaño, C., de Miguel, S., Alday, J.G., Bonet, J.A., 2022. Variations in biomass of fungal guilds are primarily driven by factors related to soil conditions in Mediterranean Pinus pinaster forests. *Biol. Fertil. Soils* 58, 487–501. <https://doi.org/10.1007/s00374-022-01621-4>.
- Hartmann, M., Brunner, I., Hagedorn, F., Bardgett, R.D., Stierli, B., Herzog, C., et al., 2017. A decade of irrigation transforms the soil microbiome of a semi-arid pine forest. *Mol. Ecol.* 26 (4), 1190–1206. <https://doi.org/10.1111/mec.13995>.
- Hedéne, P., Nilsson, L.O., Zheng, H., Gundersen, P., Schmidt, I.K., Rousk, J., Versterdal, L., 2020. Mycorrhizal association of common European tree species shapes biomass and metabolic activity of bacterial and fungal communities in soil. *Soil Biol. Biochem.* 149, 107933 <https://doi.org/10.1016/j.soilbio.2020.107933>.
- Hedéne, P., Zheng, H., Siqueira, D.P., Lin, Q., Peng, Y., Schmidt, I.K., Guldberg Frøsvlev, T., Kjeller, R., Rousk, J., Versterdal, L., 2023. Tree species traits and mycorrhizal association shape soil microbial communities via litter quality and species mediated soil properties. *For. Ecol. Manag.* 527, 120608 <https://doi.org/10.1016/j.foreco.2022.120608>.
- Ihrmark, K., Bodeker, I.T.M., Cruz-Martinez, K., Friberg, H., Kubartova, A., Schenck, J., Strid, Y., Stenlid, J., Brandström-Durling, M., Clemmensen, K.E., Lindahl, B.D., 2012. New primers to amplify the fungal ITS2 region - evaluation by 454-sequencing of artificial and natural communities. *FEMS Microbiol. Ecol.* 82, 666–677. <https://doi.org/10.1111/j.1574-6941.2012.01437.x>.
- Ishida, T.A., Nara, K., Hogetsu, T., 2007. Host effects on ectomycorrhizal fungal communities: insight from eight host species in mixed conifer-broadleaf forests. *New Phytol.* 174, 430–440.
- Jumpponen, A., Jones, K.L., Mattox, J.D., Yaeger, C., Mattox, J.D., Yaeger, C., 2010. Massively parallel 454-sequencing of fungal communities in *Quercus* spp. ectomycorrhizas indicates seasonal dynamics in urban and rural sites. *Mol. Ecol.* 19, 41–53.
- Koizumi, T., Nara, K., 2020. Ectomycorrhizal fungal communities in ice-age relict forests of *Pinus pumila* nine mountains correspond to summer temperature. *ISME J.* 14, 189–201. <https://doi.org/10.1038/s41396-019-0524-7>.
- Koizumi, T., Hattori, M., Nara, K., 2018. Ectomycorrhizal fungal communities in alpine relict forests of *Pinus pumila* on Mt. Norikura, Japan. *Mycorrhiza* 28, 129–145. <https://doi.org/10.1007/s00572-017-0817-5>.
- Kuo, S., 1996. Phosphorus. In: *Methods of Soil Analysis, Part 3: Chemical Methods*. SSSA Book Series, Madison, pp. 869–919.
- Liang, C., Schimel, J., Jastrow, J., 2017. The importance of anabolism in microbial control over soil carbon storage. *Nat. Microbiol.* 2, 17105 <https://doi.org/10.1038/nmicrobiol.2017.105>.
- Lilleskov, E.A., Hobbie, E.A., Fahey, T.J., 2002. Ectomycorrhizal fungal taxa differing in response to nitrogen deposition also differ in pure culture organic nitrogen use and natural abundance of nitrogen isotopes. *New Phytol.* 154, 219–231.
- Lin, G., McCormack, M.L., Ma, C., Guo, D., 2017. Similar below-ground carbon cycling dynamics but contrasting modes of nitrogen cycling between arbuscular mycorrhizal and ectomycorrhizal forests. *New Phytol.* 213, 1440–1451. <https://doi.org/10.1111/nph.14206>.
- Lindahl, B.D., Tunlid, A., 2015. Ectomycorrhizal fungi – potential organic matter decomposers, yet not saprotrophs. *New Phytol.* 205 (4), 1443–1447. <https://doi.org/10.1111/nph.13201>.
- Lindahl, B.D., Ihrmark, K., Boberg, J., Trumbore, S.E., Högborg, P., Stenlid, J., Finlay, R.D., 2007. Spatial separation of litter decomposition and mycorrhizal nitrogen uptake in a boreal forest. *New Phytol.* 173, 611–620.
- Lindahl, B.D., Nilsson, R.H., Tederso, L., Abarenkov, K., Carlsen, T., Kjeller, R., Kõljalg, U., Pennanen, T., Rosendahl, S., Stenlid, J., Kauserud, H., 2013. Fungal community analysis by high-throughput sequencing of amplified markers – a user's guide. *New Phytol.* 199, 288–299. <https://doi.org/10.1111/nph.12243>.
- Marron, N., Gana, C., Gerant, D., Maillard, P., Priault, P., Epron, D., 2018. Estimating symbiotic N<sub>2</sub> fixation in *Robinia pseudoacacia*. *J. Plant Nutr. Soil Sci.* 181, 296–304.
- Matsuda, Y., Kita, K., Kitagami, Y., Tanikawa, T., 2021. Colonization status and community structure of arbuscular mycorrhizal fungi in the coniferous tree, *Cryptomeria japonica*, with special reference to root orders. *Plant Soil* 468, 423–438. <https://doi.org/10.1007/s11104-021-05147-w>.
- Miranda, K.M., Espey, M.G., Wink, D.A., 2001. A rapid, simple spectrophotometric method for simultaneous detection of nitrate and nitrite. *Nitric Oxide* 5, 62–71.
- Miyamoto, Y., Nakano, T., Hattori, M., Nara, K., 2014. The mid-domain effect in ectomycorrhizal fungi: range overlap along an elevation gradient on Mount Fuji, Japan. *ISME J.* 8, 1739–1746.
- Mulvaney, R.L., 1996. Nitrogen – Inorganic forms: *Methods of Soil Analysis. Part 3*. (pp. 125–1184) Chemical Methods, SSSA, Madison, WI, USA.
- Mundra, S., Kjønaas, O.J., Morgado, L.N., Krabberød, A.K., Ransedokken, Y., Kauserud, H., 2021. Soil depth matters: shift in composition and inter-kingdom co-occurrence patterns of microorganisms in forest soils. *FEMS Microbiol. Ecol.* 97 (2021), fiab022 <https://doi.org/10.1093/femsec/fiab022>.

- Nara, K., 2006. Pioneer dwarf willow may facilitate tree succession by providing late colonizers with compatible ectomycorrhizal fungi in a primary successional volcanic desert. *New Phytol.* 171, 187–198.
- Näsholm, T., Högborg, P., Franklin, O., Metcalfe, D., Keel, S.G., Campbell, C., Hurry, V., Linder, S., Högborg, M.N., 2013. Are ectomycorrhizal fungi alleviating or aggravating nitrogen limitation of tree growth in boreal forests? *New Phytol.* 198 (1), 214–221. <https://doi.org/10.1111/nph.12139>.
- Nguyen, N.H., Song, Z., Bates, S.T., Branco, S., Tedersoo, L., Menke, J., Schilling, J.S., Kennedy, P.G., 2016. FUNGuild: an open annotation tool for parsing fungal community datasets by ecological guild. *Fungal Ecol.* 20, 241–248.
- Ochimaru, T., Fukuda, K., 2007. Changes in fungal communities in evergreen broad-leaved forests across a gradient of urban to rural areas in Japan. *Can. J. For. Res.* 37, 247–258.
- Oksanen, J., Blanchet, F., Kindt, R., Legendre, P., O'Hara, R., Simpson, G., Solymos, P., Stevens, M., Wagner, H., 2018. *Vegan: Community Ecology Package*. R Package Version 1.17-8. Available from: <http://CRAN.R-project.org/package=vegan>.
- Olsen, S.R., Cole, C.V., Watanabe, F.S., Dean, L.A., 1954. *Estimation of Available Phosphorus in Soils by Extraction with Sodium Bicarbonate*. U.S. Government Printing Office, Washington, D.C.
- Phillips, R.P., Brzostek, E., Midgley, M.G., 2013. The mycorrhizal-associated nutrient economy: a new framework for predicting carbon–nutrient couplings in temperate forests. *New Phytol.* 199, 41–51.
- Pinheiro, J., Bates, D., DebRoy, S., Sarkar, D., R Development Core Team, 2013. NLME: linear and nonlinear mixed effects models. In: R Package Version 3.1-109.
- Qiang, W., He, L., Zhang, Y., Liu, B., Liu, Y., Liu, Q., Pang, X., 2021. Aboveground vegetation and soil physicochemical properties jointly drive the shift of soil microbial community during subalpine secondary succession in southwest China. *Catena* 202, 105251.
- R Development Core Team, 2020. *R: A Language and Environment for Statistical Computing*. R Foundation for Statistical Computing, Vienna.
- Robinson, J.M., Barker, S.L.L., Arcus, V.L., et al., 2020. Contrasting temperature responses of soil respiration derived from soil organic matter and added plant litter. *Biogeochemistry* 150, 45–59. <https://doi.org/10.1007/s10533-020-00686-3>.
- Rousk, J., Brookes, P.C., Bååth, E., 2009. Contrasting soil pH effects on fungal and bacterial growth suggest functional redundancy in carbon mineralization. *Appl. Environ. Microbiol.* 75 (6), 1589–1596.
- Rousk, J., Bååth, E., Brookes, P.C., Lauber, C.L., Lozupone, C., Caporaso, J.G., Knight, R., Fierer, N., 2010. Soil bacterial and fungal communities across a pH gradient in an arable soil. *ISME J.* 4, 1340–1351.
- Santalahti, M., Sun, H., Jumpponen, A., Pennanen, T., Heinonsalo, J., 2016. Vertical and seasonal dynamics of fungal communities in boreal Scots pine forest soil. *FEMS Microbiol. Ecol.* 92, fiw170.
- Seidel, F., Lopez, C.M.L., Oikawa, A., Yamanaka, T., 2019a. Seasonal nitrogen partitioning in Japanese cedar (*Cryptomeria japonica*, D. Don) tissues. *Plant Soil* 442, 511–529. <https://doi.org/10.1007/s11104-019-04178-8>.
- Seidel, F., Lopez, C.M.L., Celi, L., Bonifacio, E., Oikawa, A., Yamanaka, T., 2019b. Tree tissues N isotope fractionation during N intra mobilization in *Fagus crenata*. *Forests* 10, 330. <https://doi.org/10.3390/f10040330>.
- Seidel, F., Lopez, C.M.L., Celi, L., Bonifacio, E., Oikawa, A., Yamanaka, T., 2022. Seasonal phosphorus and nitrogen cycling in four Japanese cool-temperate forest species. *Plant Soil* 472, 391–406. <https://doi.org/10.1007/s11104-021-05251-x>.
- Shigyo, N., Umeki, K., Hirao, T., 2019. Seasonal dynamics of soil fungal and bacterial communities in cool-temperate montane forests. *Front. Microbiol.* 10, 1944. <https://doi.org/10.3389/fmicb.2019.01944>.
- Smith, S.E., Read, D.J., 2008. *Mycorrhizal Symbiosis*, third ed. Academic Press, London, UK.
- Soudzilovskaia, N.A., van Bodegom, P.M., Terrer, C., van't Zelfde, M., McCallum, I., Luke McCormack, M., Fisher, J.B., Brundrett, M.C., de Sá, N.C., Tedersoo, L., 2019. Global mycorrhizal plant distribution linked to terrestrial carbon stocks. *Nat. Commun.* 10, 5077. <https://doi.org/10.1038/s41467-019-13019-2>.
- Steidinger, B.S., Crowther, T.W., Liang, J., et al., 2019. Climatic controls of decomposition drive the global biogeography of forest-tree symbioses. *Nature* 569, 404–408. <https://doi.org/10.1038/s41586-019-1128-0>.
- Sterkenburg, E., Clemmensen, K.E., Ekblad, A., Finlay, R.D., Lindahl, B.D., 2018. Contrasting effects of ectomycorrhizal fungi on early and late stage decomposition in a boreal forest. *ISME J.* 12, 2187–2197. <https://doi.org/10.1038/s41396-018-0181-2>.
- Taniguchi, T., Kanzaki, N., Tamai, S., Yamanaka, N., Futai, K., 2007. Does ectomycorrhizal fungal community structure vary along a Japanese black pine (*Pinus thunbergii*) to black locust (*Robinia pseudoacacia*) gradient? *New Phytol.* 173, 322–334.
- Vorříková, J., Brabcová, V., Cajthaml, T., Baldrian, P., 2014. Seasonal dynamics of fungal communities in a temperate oak forest soil. *New Phytol.* 201, 269–278.
- Wei, Y., Xiong, X., Ryo, M., Badgery, W.B., Bi, Y., Yang, G., Zhang, Y., Liu, N., 2022. Repeated litter inputs promoted stable soil organic carbon formation by increasing fungal dominance and carbon use efficiency. *Biol. Fertil. Soils* 58, 619–631. <https://doi.org/10.1007/s00374-022-01647-8>.
- Wurzburger, N., Hendrick, R.L., 2009. Plant litter chemistry and mycorrhizal roots promote a nitrogen feedback in a temperate forest. *J. Ecol.* 97, 528–536. <https://doi.org/10.1111/j.1365-2745.2009.01487.x>.
- Yang, Y., Song, Y., Scheller, H.V., Ghosh, A., Ban, Y., Chen, H., Tang, M., 2015. Community structure of arbuscular mycorrhizal fungi associated with *Robinia pseudoacacia* in uncontaminated and heavy metal contaminated soils. *Soil Biol. Biochem.* 86, 146–158. <https://doi.org/10.1016/j.soilbio.2015.03.018>.
- Zhang, Y.-L., Moser, B., Li, M.-H., Wohlgemuth, T., Lei, J.-P., Bachofen, C., 2020. Contrasting leaf trait responses of conifer and broadleaved seedlings to altered resource availability are linked to resource strategies. *Plants* 9, 621. <https://doi.org/10.3390/plants9050621>.
- Zhu, K., McCormack, M.L., Lankau, R.A., Egan, J.F., Wurzburger, N., 2018. Association of ectomycorrhizal trees with high carbon-to-nitrogen ratio soils across temperate forests is driven by smaller nitrogen not larger carbon stocks. *J. Ecol.* 106, 524–535.